

FEM analysis of stress Predication of Aluminum wire rod in Drawing Operation

Bhimsen Moharana¹, Bashishth Kumar Kushwaha²

¹DR. B.B.A Government Polytechnic, Karad D.P, Silvassa, India

²Roorkee Engineering & Management Technology Institute, Shamli, India

Abstract - The quality of drawn wire and breakage during drawing operation is a function of various factors, such as die pass schedule and die details, wire rod properties, machine parameters like cooling and lubrication of dies and drum etc. An attempt is made by the investigator to trace their stresses and strain to suggest viable corrective/preventive measures. In this work simulation results for stress and strain analysis for different condition of lubrication revealed the plastic stress and strain values during plastic deformation of wire materials have been analyzed. With higher value of friction co-efficient local stress and strain causes surface failure leading to damage of wire surface and breakage. Friction value of 0.10 was found to be most suitable for all die stations against surface failure and breakage.

Keywords: Cold forming, rolling, wires drawing, defects origin, flow patterns, FEA model analysis

1. INTRODUCTION

A cable is two or more wires running side by side and bonded, twisted, or braided together to form a single assembly. Electrical cable is an assembly consisting of one or more conductors. Aluminium and its alloy conductors are preferred and dominant for cable in several areas of power transmission and distribution. The major areas dominant by aluminium and its alloys cables are non-insulated overhead power transmission, insulated overhead power transmission and distribution. It is because of its strength to weight ratio and cost with respect to copper, though its conductivity is about 60% of that of copper.

The effects of process parameters such as the cooling condition of the work-rolls, the rolling speed, and the roll metal interfacial heat-transfer coefficient on the temperature distributions in the work-rolls as well as in the rolling metal. The comparison between the model predictions and experimental results shows the validity of the proposed model [1]. 3-D finite element analysis for single pass and multi-pass wire drawing in order to evaluate the deformation behavior of various surface defects having different aspect ratio. They found that the numerical simulations results match well with experimental results for introduced of any arbitrarily longitudinal, transverse, oblique and round defects possibly formed during both of the wire drawing process [2]. Metallographic observation on polished samples gives key information on surface defect origin on carbon steel bar and wire using several reagents. They also

observed pin holes on billet due to sand blasting, on rolling may disappear due to scale formation for small holes and get elongated in rolling direction for larger holes. They found that transverse cracks in billet, during rolling with high reduction ratios creating longitudinal defects [3]. Industrial experiments in a steel company and suggested that the removal of defects is either performed selectively by removing the specific defect on the surface specific to the semi-finished products continuously cast. They suggested discovering the generating source of inclusions during casting and rolling operations to take the proper measures and take remedy where appropriate for preventing failure in subsequent drawing operation [4].

The temperature of H-beam was a downward trend in the hot rolling process, however, local temperature display rising trend, uneven deformation of flange lead to more complex temperature distribution, there is certain correlation between equivalent plastic stress and temperature distributions, increasing of equivalent plastic stress as the temperature increases, research results can provide theoretical basis for rolling regulations and reference of the production of hot rolling for H-beam [5-8]. A series of different metallic materials, diameters and production environment by scanning electron microscopy and conical microscopy analyzed. With the image of the structure for the surface quality of the metallic wire, a nomenclature and cause for each surface defect is proposed. The catalogue of surface defects creates a basis for developing instruments for measuring surface quality of wire for checking the breakage of wire in subsequent drawing operation [9]. The effect of several geometry parameters on the wire drawing process using a 5052 aluminium alloy considering strain hardening damage studied. They obtained that, within the study interval, the most significant effect on the plastic deformation is the section reduction, followed by the semi-cone angle of the die and the friction coefficient although this to a lesser degree. They also found a high value of plastic deformation in the material can lead to an excessive level of damage inside the wire. The accumulated damage mainly depends on the semi-cone angle of the die and to a lesser extent, on the percentage of section reduction, being the effect of the friction coefficient very low [10]. The analytically and numerically the parameters affecting wire drawing process using a 3D finite element model DEFORM-3D V6.1 and material aluminium-1100 for simulation investigated. They found that the increasing in bearing length causes an increase in the drawing force and to avoid the increase

drawing force, the reduction in area and friction coefficient should be small with a large die angle. They also observed that with certain range of velocities, drawing force decreases with increase in velocity and failure takes place when the velocity goes out of this range [11]. The influence of the microstructure on the physico-mechanical properties of Al-Mg-Si alloy. The alloy was nano-structured using severe plastic deformation by high pressure torsion at different deformation range investigated. They found ultrafine grain structure with nano-inclusions of secondary phases and an excellent combination of high strength and electrical conductivity [12].

Metallurgical investigation of different causes of center bursting led to wire breakage during production carried out. They found with experimental observations that grain flow, porosity and internal cracks etc in material leading to metallurgical defects in raw material and cause material failure. They also observed the presence of hard brittle phase which makes the central fibers brittle and create center bursting in wires. The central bursting formation in wires led to wire breakage [13].

The experimental work to predict the formation of chevron crack in copper wire drawing process, found the chevron crack formation initiated by a central burst inside the wire material using experimental tests. The results when compared with the results from a series of numerical simulations using the Cockcroft–Latham fracture criterion, found in the conditions of central burst formation along the wire axis, depending on drawing parameters and friction coefficient between the die and the wire. The friction coefficient is a linear function of temperature rise which is measured close to the wire die interface [14]. The formation of edge defects in hot strips, resulting from slab corner cracks generated in continuous casting. They developed a model-based concepts for the identification of such initial slab cracks. To accomplish this task a systematic finite element tool Deform-3D was utilized. The numerical results clearly pointed out the significant morphological changes of the cracks during rolling and afford valuable indications for a deeper understanding of the underlying process details [15-17]. The old drawing device had the problems of low stiffness of the guiding die and of short service time of peeling die with poor roughness of peeled wire surface. They proposed a multi-step process which includes front guiding, drawing, peeling, redrawing and rear guiding. Based on the principle of metal cutting and researched results, it was found, the peeling-redrawing die that had a long durability and improved the wire surface quality after peeled and redrawn [18]. They observed necking on the wire containing an inclusion and maximum hydrostatic tensile stress occurred on wire centerline in front of inclusion for single-pass drawing. When the wire was repeatedly drawn, the maximum hydrostatic tensile stress regions symmetrically separated out and were at both side of wire centerline in front of inclusion [19]. The influence of casting parameters on casting conditions and interference of casting parameters on the final strip characteristics such as constant strip

thickness, surface quality and roughness of aluminum alloys sheet 6.30 to 6.50 mm thick. They also found that casting speed, roll force and roll gap should have the greatest influence on the final strip thickness and the examined parameters agree well with the theoretical values [20]. J-integral value increased with the increasing of the angle of drawing die, the friction coefficient between drawing die and wire and the initial dimension of the flaw. When friction coefficient equaled 0.1, J-integral value round the crack tip with the same flaw decreased with the decreasing of the angle of the die. J-integral value changed slightly and tended to be a constant value when the angle reached to 8°. They found that maintaining low friction and best pull out angle of dies, rate of breakage of wire can be reduce in production process [21]. Deformation characteristic of low carbon steel under hot compression conditions at the temperature range of 650–1000°C using Gleeble 3800 thermo-mechanical simulator for the formation of micro-cracking observed. They found the change of microstructures using an optical microscope. The hot deformation process was numerically simulated using finite element technique to determine the local strain, strain rate, and temperature distributions. They also observed the microstructure changed quite differently after the deformation at various temperature levels. The grain size and shape were also varied during the deformation process depending on the characteristics of metal flow. The initiation of micro-crack was found to be strain and temperature dependent. Such a micro-cracking was easy to initiate at the position with high stress and strain, especially at the grain sliding boundaries [22]. They developed illumination system with blue LED lighting sources to get best quality of surface image and implemented defect detection algorithms based on block sigma transform which can recognize wire rod objects and segments defect from the images in robust and efficient manner [23]. Drawing operation using ANSYS found that provision of die land and fillet at die entry made the material flow smooth, less stress and low heat generation analyzed. Hence least wire defect drawing defects and wire breakage [24].

The role of residual stresses on wire fracture strength in drawing operation using 5052 aluminium alloy observed. They found that maximum value of axial stress increases when the semi-cone angle of the die increases or cross section area reduction decreases. They also found that compressive residual stresses reduce crack growth but tensile residual stresses on the surface of the wire causes more damage [25]. The wire drawing process of polycrystalline diamond (PCD) wire drawing die using ABAQUS FEA software for drawing solar wafer cutting wire and obtained a maximum stress of die blank to find the drawing force studied. The investigators analyze the effect of different reduction angle on drawing force on same PCD die. From the experiment the investigators concluded that for the reduction of drawing force and the equivalent stress of PCD shaper hole, the reduction angles of shaper hole should be set in the range of 7°-8° [26]. The damage evolution of the drawn wire in each of the eight passes and observed the damage distribution along axial and circular directions. Wire

breakage expected to occur in those areas of the drawn wire where fractures most possibly initiate. They found damage evolution on the surface of the wire due to sticking friction [27]. The calculation of lubricant film thickness with drawing parameters and concluded that lubricant film thickness increases when die angle increases. Lubricant not only improves the surface finish of the product but also act as heat insulation between the billet and the die. He also suggested that a lubricant selected for drawing operation will not shear too easily and chance of failure or rupture of wire with high viscosity lubricants [28]. Microstructure evaluation of FSW joints clearly shows the formation of new fine grains and refinement of reinforcement particles in the weld zone with different amount of heat input by controlling the welding parameter [29-30]. The lubricant concentration in the emulsion used in wire drawing control the friction and wearing of contact surfaces. They found that change in emulsion concentration for certain lubricant influences friction parameters as well as wear parameters in the process of wire drawing and control the speed of wire drawing through the matrix [31]. The vibration behavior of wire in wire drawing process was observed. They found that wear profile and generation of ringing on die is due to the effect of wire vibration. It was also observed that simulation Abaqus FEA result and experimental result are same. Thus they concluded that simulation can be used to accurately predict the die wear profile [32]. FEM tool designed to simulate wire drawing can generate practical information for the analysis and optimization of output wire properties concluded. The possibility of central burst can be analyzed by looking at the tri-axiality of the stress state on the central line or as accumulated damage [33]. A failure analysis procedure of steel wire drawing using metallographic examination and microscopic analysis and found that fracture modes are corresponded to macro fracture morphology and surface state of wire [34].

2. PROBLEM DESCRIPTION

The aim of this work is to understand the cause of defects leading to breakage during wire drawing operation for aluminum alloy cable. The wire material was Al-Mg-Si alloy of grade 6201. The breakage of wire during drawing operation occurs sometimes in random. Since the breakage of wire during the drawing operation is a random error the breakage samples of wires for input wire rod as well as processing wire of intermediate dies stations are under investigation for their causes and effects. Metallurgical limitation in input wire rod material for porosity, internal cracks and inclusions are to be studied. Wire tensile failure mode is also verified from flow stress to draw stress ratio taking die geometry and friction condition into consideration. Since random breakage is the subject of study, simulations for different friction condition are carried out for an optimum result. CAD models are developed for study the wire stresses, strains, die stresses and temperature for critical dies stations for predicting defects in wire. ANSYS LS-DYNA is used for the analysis purpose.

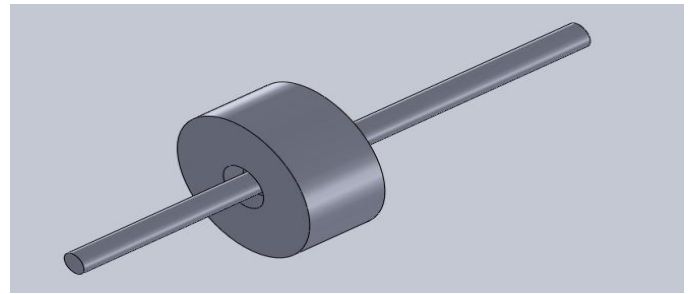


Fig. 1: 3D CAD model for die and wire assembly for die no.5

3.1 Material Properties

Table 1: Material properties for wire rod

| | |
|----------------------------------|--|
| Wire material density (ρ) | = $2.74 \times 10^{-3} \text{ Kg/m}^3$ |
| Young's modulus (E) | = $7.03 \times 10^{10} \text{ N/m}^2$ |
| Poisson's ratio (μ) | = 0.34 |
| Rigidity modulus (G) | = $2.5 \times 10^{10} \text{ N/m}^2$ |
| Bulk modulus (K) | = $7.5 \times 10^{10} \text{ N/m}^2$ |
| Thermal conductivity (K_t) | = 244 W/mK |
| Specific Heat (C_p) | = $875 \text{ J.Kg}^{-1}\text{K}^{-1}$ |

Table 2: Material properties for Poly Crystalline Dies:

| | |
|---------------------------------|--------------|
| Die material density (ρ) | = 3.43 gm/cc |
| Compressive Stress | = 4.74 GPa |
| Fracture toughness | = 6.89 Mpa/m |
| Young's modulus (E) | = 925GPa |
| Poisson's ratio (μ) | = 0.086 |
| Rigidity modulus (G) | = 426GPa |
| Bulk modulus (K) | = 372GPa |
| Thermal conductivity (K_t) | = 120 W/m K |

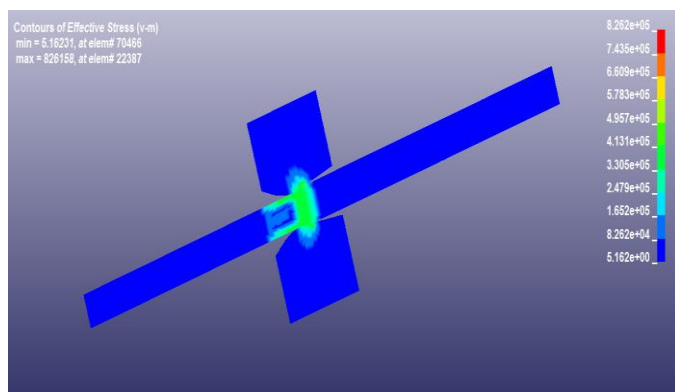
3. RESULT AND DISCUSSION

Aluminium wire drawing is a cold working plastic deformation process. The wire passes through a series of dies where compressive stresses act along the two axes and tensile stress along the third axis. The plastic deformation in the metal takes place only when the applied stress level exceeds the yield stress but less than the fracture strength of the metal. Thus for successful wire drawing operation the drawing stress should never exceed the flow stress. If material composition is not uniform and voids or slag inclusion present in the material, then fracture strength is uncertain and it leads to breakage of wire rod in drawing operation. Friction plays an important role in wire drawing operation with reference to surface defects and subsequent wire breakage. With very high value of co-efficient of friction, sticking action of wire material to die causes surface defects

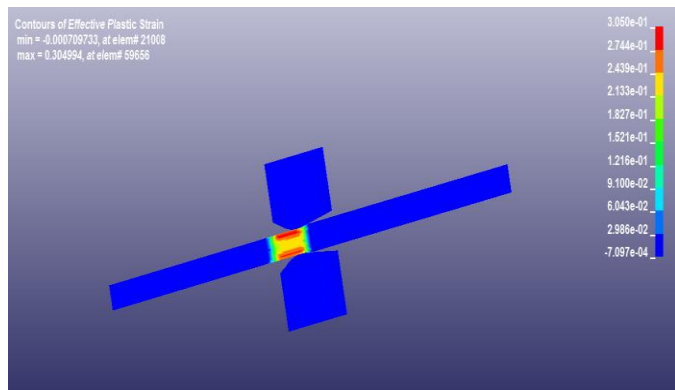
and with very low value of friction it will produce very dull, lumpy and matte surface, unsuitable for electrical conductor[27]. So it is desirable to find the optimum value of coefficient of friction for defect free cable production through simulation result.

3.1 Simulation Results in Die Stage No.3 ($\mu=0.20$)

When the wire in die stage No.3 was subjected to simulation under friction co-efficient 0.20, the maximum effective plastic stress produced was 826.158 MPa, at element 22787 and maximum effective plastic strain was 0.3049994 at element 59656 as shown in the fig.2. (a) and (b). Local strain development in wire material at different deformed parts is also represented in different colors as shown in status bar.



(a)

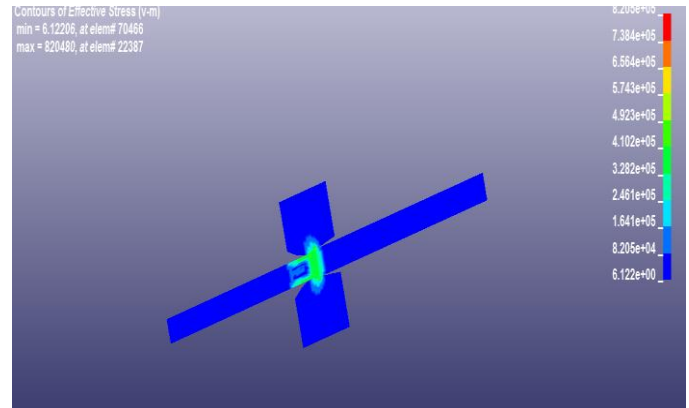


(b)

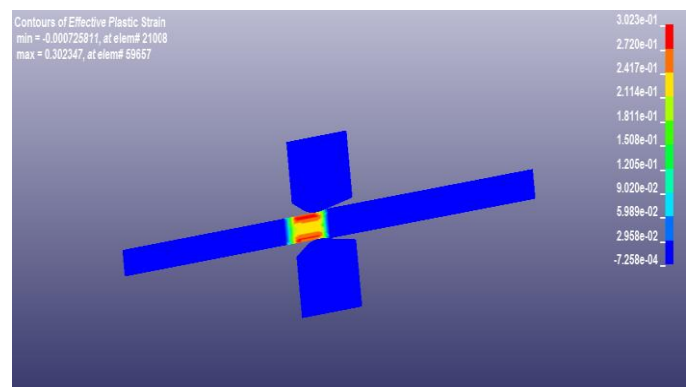
Fig. 2 : Effective (a) stress (b) strain in wire stage no.3 ($\mu=0.20$)

3.2 Simulation Results in Die Stage No.3 ($\mu=0.15$)

When the wire of diameter 6.38 mm for die stage No.3 was subjected to simulation under friction co-efficient 0.15, the maximum effective plastic stress produced was 820.480 MPa, at element 22387 and maximum effective plastic strain was 0.302347 at element 59667 as shown in the fig.3 (a) and (b). Local strain development in wire material at different deformed parts is also represented in different colors as shown in status bar.



(a)

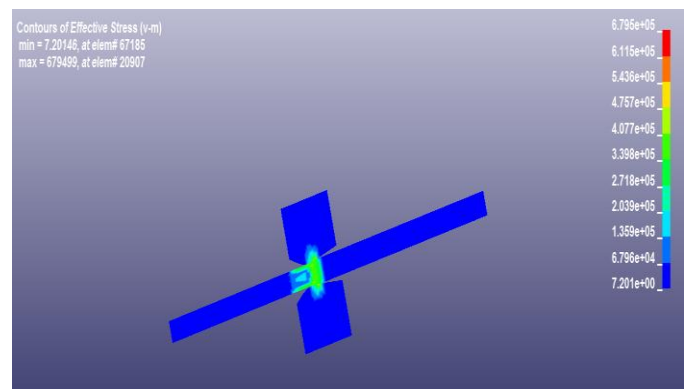


(b)

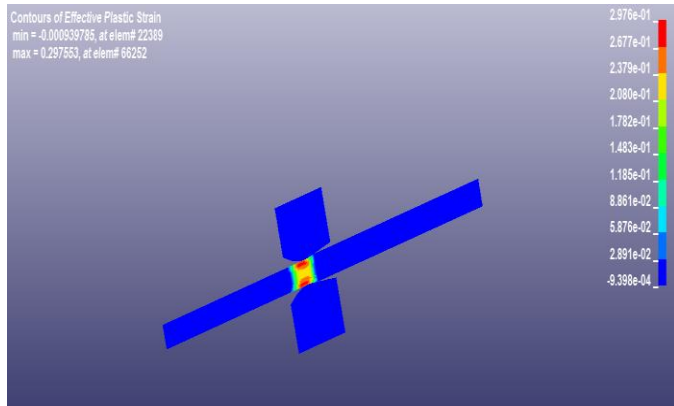
Fig. 3: Effective (a) Stress (b) Strain In Wire Stage No.3 ($\mu=0.15$)

3.3 Simulation Results in Die No.3 ($\mu=0.10$)

When wire of diameter 6.38 mm for die station No.3 was subjected to simulation under friction co-efficient 0.10, the maximum effective plastic stress produced was 679.499 MPa at element 20907 and maximum effective plastic strain was 0.297553 at element 66252 as shown in the fig.4 (a) and (b). Local strain and stress development in wire material at different deformed parts are also represented in different colors as shown in status bar.



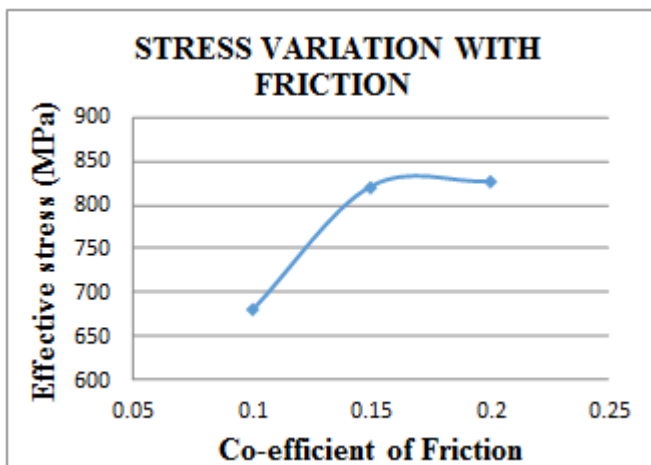
(a)



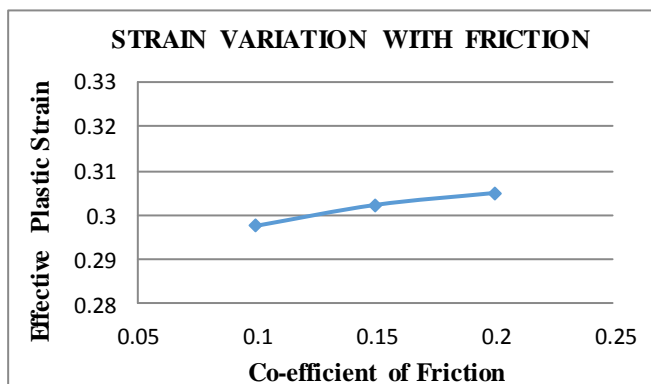
(b)

Fig. 4: Effective (a) Stress (b) Strain in Wire Stage No.3 ($\mu=0.10$)

The effective plastic stress and plastic strain results obtained for wire rod of diameter 6.38 mm with co-efficient of friction values 0.20, 0.15 and 0.10 are plotted in the form of graph as shown in fig. 5 (a) and (b).



(a)

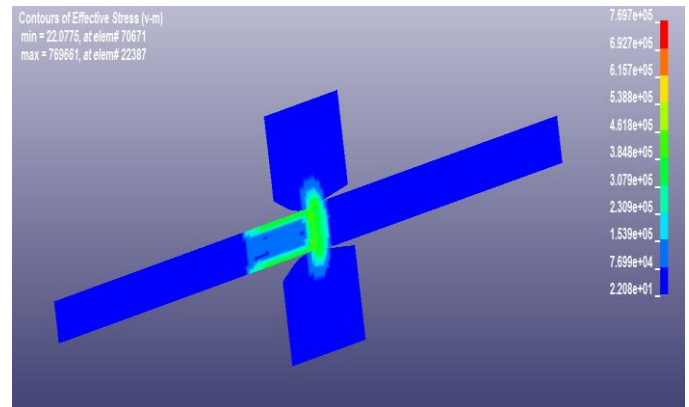


(b)

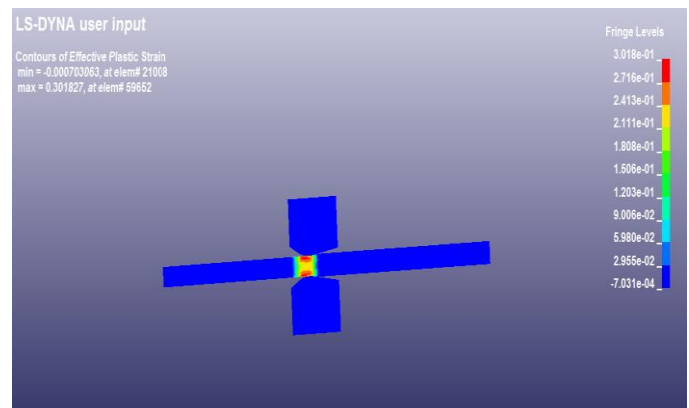
Fig. 5: (a) Stress and (b) Strain with Friction in Wire Stage No.3

3.4 Simulation Results in die No.4 ($\mu=0.14$)

When the wire of diameter 5.69 mm for station No.4 was subjected to simulation under friction co-efficient 0.14, the maximum effective plastic stress produced was 769.661 MPa at element 2238 and maximum effective plastic strain developed was 0.301827 at element 59652 as shown in the fig.6 (a) and (b). Local strain and stress development in wire material at different deformed parts are also represented in different colors as shown in status bar.



(a)

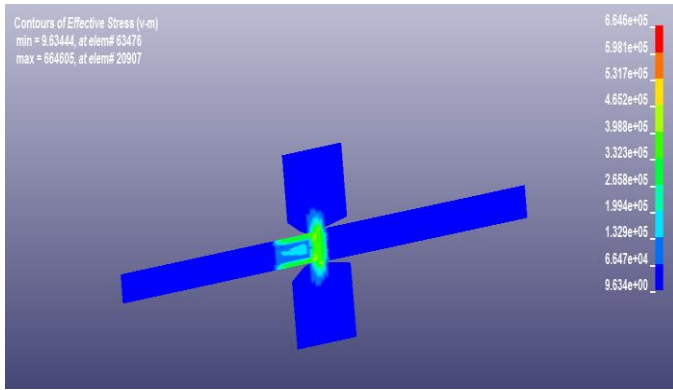


(b)

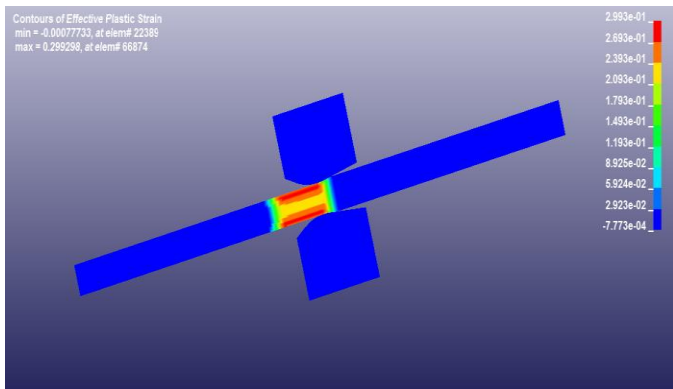
Fig. 6: Effective (a) stress (b) strain in wire stage no.4 ($\mu=0.14$)

3.5 Simulation Results in Die No.4 ($\mu=0.10$)

When the wire of diameter 5.69 mm for station No.4 was subjected to simulation under friction co-efficient 0.10, the maximum effective plastic stress produced was 664.606 MPa and maximum effective plastic strain developed was 0.299298 as shown in the fig.7. (a) and (b). Local strain and stress development in wire material at different deformed parts are also represented in different colors as shown in status bar.



(a)

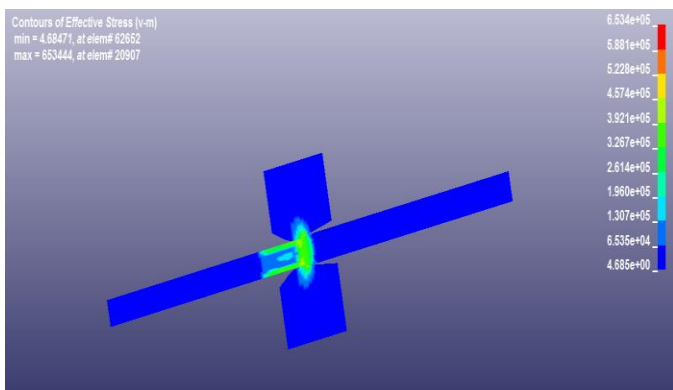


(b)

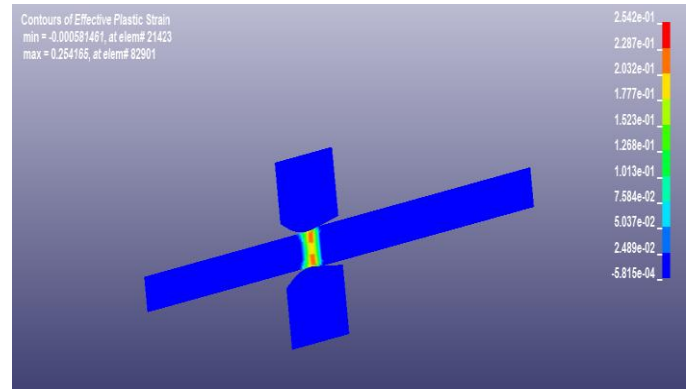
Fig. 7: Effective (a) stress (b) strain in wire stage no.4 ($\mu=0.10$)

3.6 Simulation Results in Die No.4 ($\mu=0.08$)

When the wire of diameter 5.69 mm for die station No.4 was subjected to simulation under friction co-efficient 0.08, the maximum effective plastic stress produced was 653.444 MPa at element 20907 and maximum effective plastic strain developed was 0.284166 as shown in the fig.8 (a) and (b). Local strain and stress development in wire material at different deformed parts are also represented in different colors as shown in status bar.



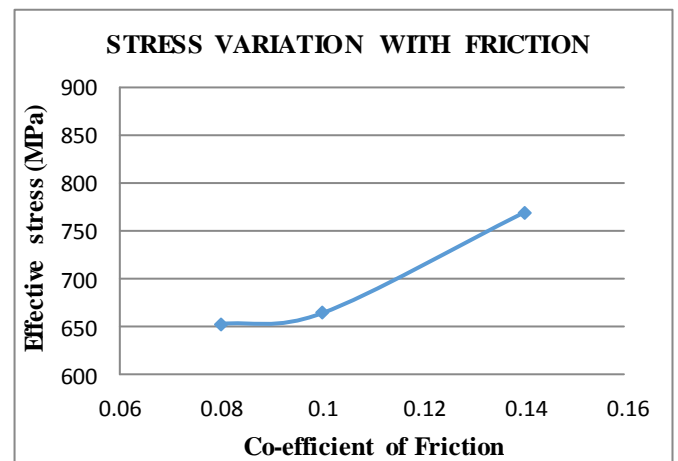
(a)



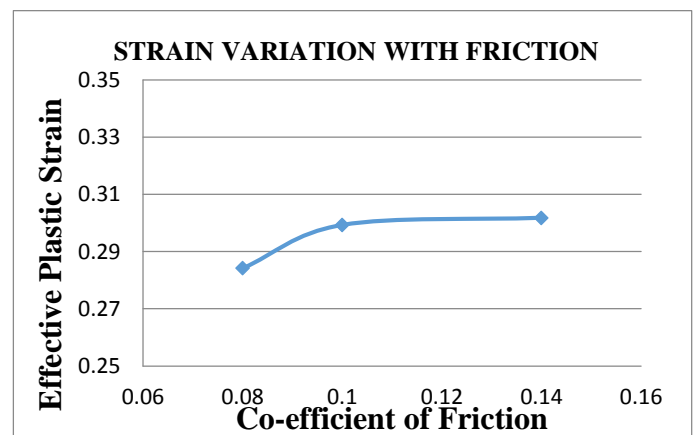
(b)

Fig. 8: Effective (a) stress (b) strain in wire stage no.4 ($\mu=0.08$)

The effective plastic stress and plastic strain results obtained for wire rod of diameter 5.69 mm with co-efficient of friction values 0.15, 0.10 and 0.08 are plotted in the form of graph as shown in fig.9 (a) and (b).



(a)

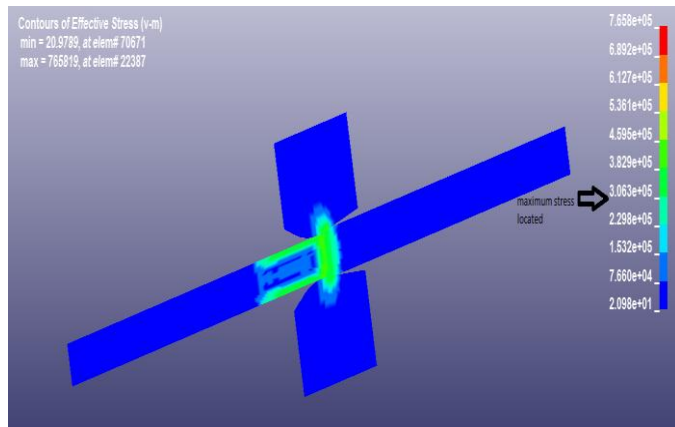


(b)

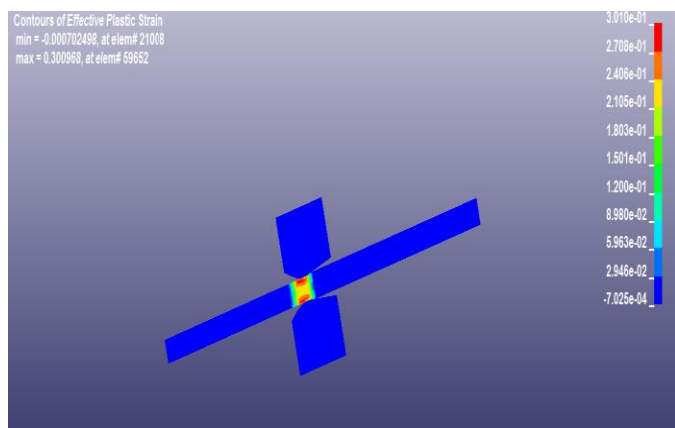
Fig. 9: (a) stress (b) strain with friction in wire stage no.4

3.7 Simulation Results for Die No.5 ($\mu=0.12$)

When the wire of diameter 5.06 mm for die station No.5 was subjected to simulation under friction co-efficient 0.12, the maximum effective plastic stress produced was 765.819 MPa, and maximum effective plastic strain produced was 0.300968 as shown in the fig. 10 (a) and (b) Local strain and stress development in wire material at different deformed parts are also represented in different colors as shown in status bar.



(a)

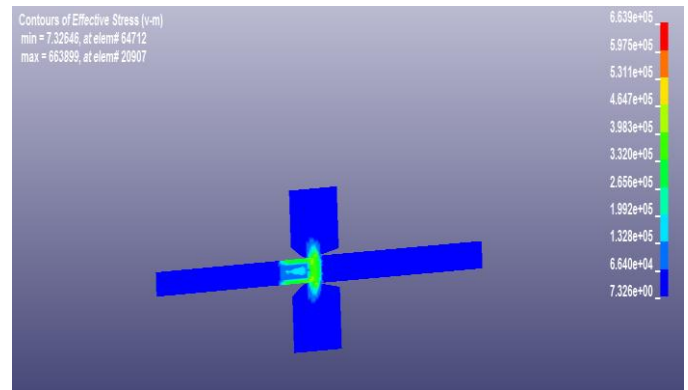


(b)

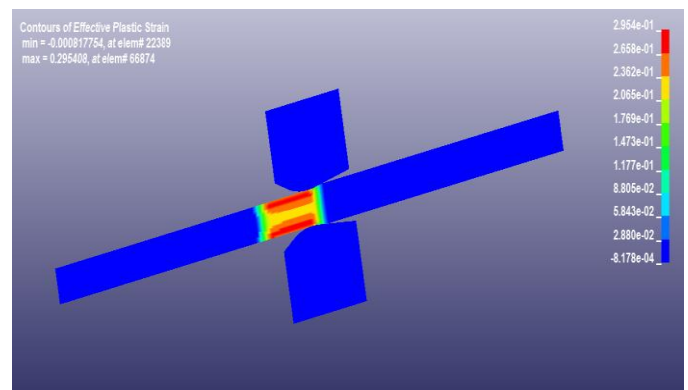
Fig. 10: Effective (a) stress (b) strain in wire stage no.5 ($\mu=0.12$)

3.8 Simulation Results in Die No.5 ($\mu=0.10$)

When the wire of diameter 5.06 mm for die station No.5 was subjected to simulation under friction co-efficient 0.10, the maximum effective plastic stress produced was 663.899 MPa and maximum effective plastic strain was 0.295408 in wire as shown in the fig.11 (a) and (b). Local strain and stress development in wire material at different deformed parts are also represented in different colors as shown in status bar.



(a)

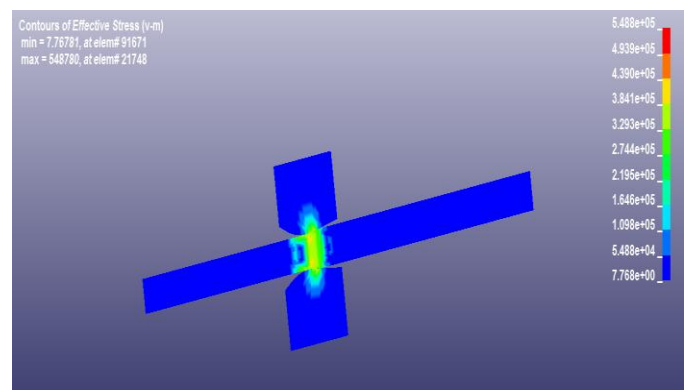


(b)

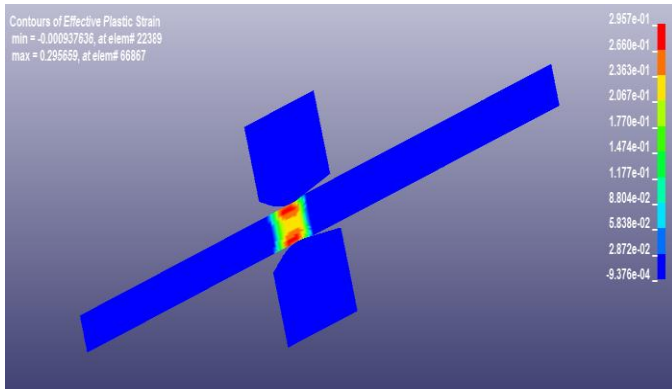
Fig. 11: Effective (a) stress (b) strain in wire stage no.5 ($\mu=0.10$)

3.9 Simulation results for die No.5 ($\mu=0.06$)

When the wire of diameter 5.06 mm for die station No.5 was subjected to simulation under friction co-efficient 0.06, the maximum effective plastic stress produced was 548.78 MPa and maximum effective plastic strain was 0.295659 as shown in the fig. 12 (a) and (b). Local strain and stress development in wire material at different deformed parts are also represented in different colors as shown in status bar.



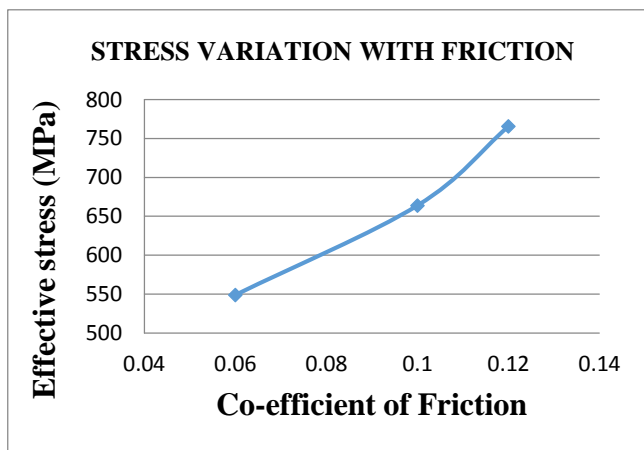
(a)



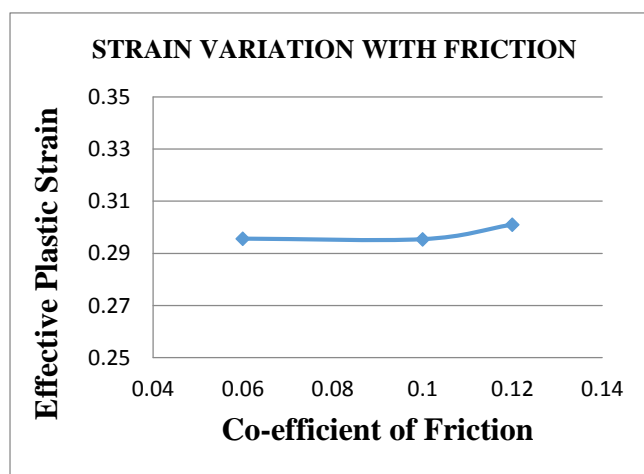
(b)

Fig. 12: Effective (a) stress (b) strain in wire stage no.5 ($\mu=0.06$)

The effective plastic stress and plastic strain results obtained for wire rod of diameter 5.06 mm with co-efficient of friction values 0.20, 0.15 and 0.10 are plotted in the form of graph as shown in fig.13 (a) and (b).



(a)



(b)

Fig. 13: (a) stress (b) strain with friction in wire stage no.5

The result obtained during simulations of all the above three die stations are summarized in Table 3

Table 3: simulation results with varying friction coefficients

| Die Stage No. | Friction Coeff (μ) | Effective Plastic Stress(Von-Mises), MPa | Effective Plastic Strain |
|--|--------------------------|--|--------------------------|
| D 3 Initial Wire Dia.6.38 mm Final Wire Dia. 5.69 mm | 0.2 | 826.16 | 0.305 |
| | 0.15 | 820.48 | 0.3023 |
| | 0.1 | 679.5 | 0.2976 |
| D 4 Initial Wire Dia. 5.69mm,Final Wire Dia.5.06 mm | 0.14 | 769.66 | 0.3018 |
| | 0.1 | 664.61 | 0.2993 |
| | 0.08 | 653.44 | 0.2842 |
| D 5 Initial Wire Dia.5.06 mm Final Wire Dia. 4.51mm | 0.12 | 765.82 | 0.301 |
| | 0.1 | 663.9 | 0.2954 |
| | 0.06 | 548.78 | 0.2956 |

3.10 Analysis of Friction Effect on Wire Breakage

Wire drawing process is a metal deformation process which is subjected to uni-axial tension and biaxial compression in a die. In this section, the effect of the change in the coefficient of friction on stress and strain resulting from the deformation is discussed.

In wire drawing, a break occurs when the draw stress (σ_d) equal the flow stress (σ_f) of the material at die exit i.e. $\frac{\sigma_d}{\sigma_f} = 1$. Yielding and breaking are generally associated

because of plastic stretching of wire between dies. It is observed practically that wire breaks become frequent at a ratio of draw stress to flow stress less than one despite the wire being not containing obvious flaws. In high productivity operation the ratio of draw stress to flow stress is cited as 0.7 to be the practical maximum to avoid wide spread flow growth and frequent breakage.

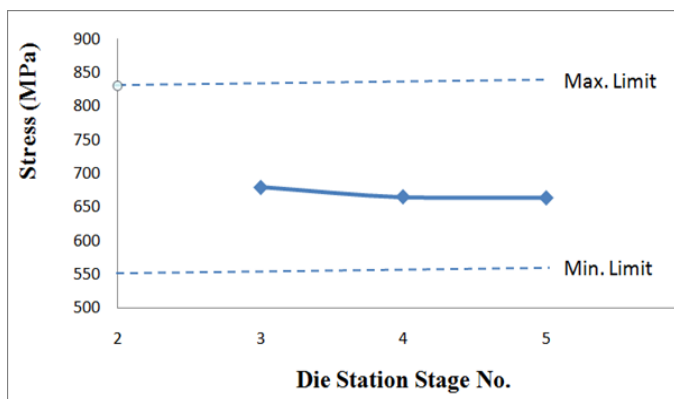
The ratio of draw stress to flow stress is a function of die shape, die angle and co-efficient of friction. Since there was a constraint on varying the die shape factor and die angle during the present work, the co-efficient of friction was the major factor to be determine for avoiding wire breakage. Keeping in view the constraint on maintaining the ratio of draw stress to flow stress (less than one or preferably equal 0.7), the maximum co-efficient of friction in the present work to be considered was 0.20, for which the ratio of draw stress to flow stress is 0.75.

In drawing operation as the diameter of wire decreases along the successive die stages, the drawing speed increases

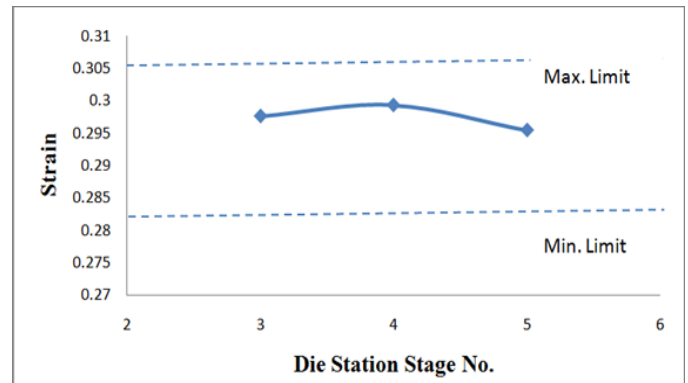
as per the continuity equation. Accordingly, the co-efficient of friction may be highest at the first die station and decreases on successive die stations. As the co-efficient of friction decreases, the thickness of lubrication film around the wire increases. Due to this, the ironing effect of die on the wire being drawn is substantially reduced and the wire material has space for lateral straining. This results in a dull or matte surface of wire, which is undesirable for electrical application. Therefore the minimum value of coefficient of friction consider for the present problem was 0.06.

It is desirable that the maximum effective plastic stress as well as plastic strain should be on the lower side and uniform in drawing operation. The stress- strain analysis of wire drawing operation at die stage D₃, D₄ and D₅ revealed the effective plastic stress and plastic strain values for different co-efficient of friction. In die stage D₃, the minimum plastic stress (679.50 MPa) and minimum plastic strain (0.2976) were obtained for co-efficient of friction 0.10. In die stage D₄, the minimum plastic stress and plastic strain values were obtained for co-efficient of friction 0.08. However for co-efficient of friction 0.10 in D₄, the plastic strain was 0.2993, which was closer to the plastic strain value for co-efficient of friction 0.10 in die stage D₃. Further for the friction value 0.10 in die stage D₄, the stress was 664.61 MPa which was marginally (0.72%) higher than that obtained for friction value 0.08. Also this stress value was closer to the plastic stress obtained in die stage D₃ for co-efficient of friction 0.10.

In die stage D₅, the minimum value of plastic strain (0.2954) was obtained for friction co-efficient 0.10 for which the effective plastic stresses was 663.90 MPa. Therefore it was observed that desirable value of effective plastic stress as well as plastic strain in die stage D₃, D₄ and D₅ corresponded to friction co-efficient 0.1. For this value of co-efficient of friction, the ratios of draw stress to flow stress obtained were 0.53, 0.33 and 0.31 for die stages D₃, D₄ and D₅ respectively. The stress and strain plots for all the three die stages for friction value 0.10 is shown in fig.14 are fairly in narrow region and towards lower value of the stress and strain.



(a)



(b)

Fig. 14: (a) stress (b) strain with friction ($\mu=0.10$)

Hence the coefficient of friction value 0.10 is preferred considering the constraint of draw stress to flow stress ratio.

4. RECOMMENDATIONS

The random breakage of 6201 Al-Mg-Si alloy wire rod during drawing operation through rod break down (RBD) machine was analyzed. During metallurgical investigation of wire rod, large size of secondary precipitation elements like Mg and Si were found. These are in form of hard spinels or foreign inclusions, randomly distributed throughout the wire. Since hard inclusions are the cause of wire breakage, it is suggested that during metallurgical activity in the furnace for alloying, care should be taken for homogenization of the secondary particles and their size through proper mixing and intensive filtration activity such as electro-slag refining. Furnace liner particles, creating foreign inclusions are also taken into consideration with due metallurgical sample verification.

Lubrication activity in the wire drawing was found for the cause of random breakage as it controls the friction parameters in wire-die interface. It was found high coefficient of friction above 0.10, created during plastic stretching of wire make the draw stress to flow stress ratio beyond 0.60 in tensile failure analysis. The friction value of 0.10 was found suitable for all die stations to avoid random breakage due to the anisotropic behavior of wire material. Simulation results show different values of plastic stresses and strain during plastic deformation of wire materials. With higher value of friction co-efficient, local stresses and strain causes surface failure leading to damage of wire surface and breakage. Friction value of 0.10 found to be most suitable for all die station against surface failure and breakage.

Thus it is suggested that in order to avoid the random breakage of wire during drawing operation in the RBD machine, the following key points are to be implemented:

1. Defects in wire stock such as voids or lamination or inclusions may be avoided using proper metallurgical treatment. The wire rod can be monitored through any NDT testing process like online radiography test.

2. Insufficient lubrication causes increased friction leading to wire breakage. So co-efficient of friction value of 0.10 may be maintained for all the die stations.
3. The operator should not set the die in the wrong direction through the die block during die setting and proper die alignment is to be verified.
4. Care should be taken that wire stock is not tangled on feed side of draw die.

5. CONCLUSION

Simulation results for stress and strain analysis for different condition of lubrication revealed the plastic stress and strain values during plastic deformation of wire materials. With higher value of friction co-efficient local stress and strain causes surface failure leading to damage of wire surface and breakage. Friction value of 0.10 was found to be most suitable for all die stations against surface failure and breakage.

REFERENCES

- [1] Myung-Sik Chun, Ick-Tae Ahn, and Young-Hoon Moon, "Deformation Behavior of a Slab with Width Reduction in a Hot Mill" JMEPEG, 2005, pp. 408-412.
- [2] Baek, M. H, Jin, G.Y, Hwang, K.S, Im, T.Y and Lee, D.L. (2011). "Numerical study on the evolution of Surface Defects in Wire drawing" Journal of Material processing Technology 212 (2012), 776-785
- [3] Dekate, D., Deshmukh, B.D. and Khedkar, S. (2013). "Study and Minimization of Surface Defects on Bars and Wire Rod Originated in Continuous Cast Billets" International Journal of Modern Engineering Research (IJMER), Vol 3, 736-738
- [4] Erika Monica, P. and Imre, K. (2010). "Assessment of Surface Defect in the Continuous Cast Steel" Bulletin of Engineering, Tome IV 109-115.
- [5] Xianzhang FENG, Junwei CHENG, Cai LIU, Junhui LI and Yanmei CUI, "Simulation of Mechanics Properties in Rolling Process for H-beam", International Joint Conference on Artificial Intelligence, 2009, pp.719-722.
- [6] Manoj Saini , Navneet Arora , Chandan Pandey, Husain Mehdi, Mechanical Properties of Bimetallic Weld Joint between SA 516 Grade 65 Carbon Steel and SS 304 L For Steam Generator Application, International Journal of Research in Engineering and Technology, Vol 3(7) 2014, 39-42.
- [7] Manoj Saini , Navneet Arora , Chandan Pandey, Husain Mehdi, Preliminary Studies on Thermal Cycling of Reactor Pressure Vessel Steel, International Journal of Mechanical Engineering, Vol 4 (2), 2014, 51-58.
- [8] Husain Mehdi, Shwetanshu Gaurav Teetu Kumar, Prasoon Sharma, Mechanical Characterization of SA-508Gr3 and SS-304L Steel Weldments, International Journal of Advanced Production and Industrial Engineering vol 2, issue 1, 2017, 41-46.
- [9] Bernabeu, E., Sanchez-Brea, L. M., Siegmann, P. and Hermann, H.(2001). "Classification of Surface structures on Fine Metallic Wires" Applied Surface science 180 (2001) 191-199
- [10] J. León, C.J. Luis, D. Salcedo, R. Luri, I. Puertas, I. Pérez (2010). "Effect of the Die geometry on the Imparted Damage in Wire Drawing" Trends in the Development of Machinery and Associated Technology TMT 2010, 73-66
- [11] Hassan F. Abdul Kareem, Hashim S. Alyan (2015). "Three dimensional finite element analysis of wire drawing process" University journal of Mechanical Engineering, 3(3)71-82
- [12] Mavlyutov, A. M, Kasatkin, I.A, Valiev, R.Z and Orlova, T. S. (2015). "Influence of the microstructure on the physic-mechanical properties of the aluminum alloy Al-Mg-Si nano-structured under sever plastic deformation" Physics of the Solid State, 2015, Vol. No.10, pp. 2051-2058
- [13] Das Souvik, Mathura Jitendra, Bhattacharyya Sandip (2013). "Metallurgical Investigation of different causes of center bursting led to wire breakage during production" Case Studies in Engineering Failure Analysis, (2013), 32-36.
- [14] Haddi, A., Imad, A. and Vega, G. (2012). "The influence of the drawing parameters and temperature rise on the prediction of chevron crack formation in wire drawing" Int J Fract (2012) 176:171-180.
- [15] Alexander Kainz, Sergiu Ilie, Erik Parteder and Klaus Zeman, "From Slab Corner Cracks to Edge-Defects in Hot Rolled Strip, Experimental and Numerical Investigations", Steel Research International, Vol.79, February, 2008, pp. 861-867.
- [16] Husain Mehdi Rajan Upadhyay, Rohan Mehra, Adit, Modal Analysis of Composite Beam Reinforced by Aluminium-Synthetic Fibers with and without Multiple Cracks Using ANSYS, International journal of Mechanical Engineering, vol-4 issue-2, pp 70-80, 2014.
- [17] Husain Mehdi, Anil Kumar, Arshad Mehmood, Manoj Saini, Experimental Analysis of Mechanical Properties of Composite Material Reinforced by Aluminium-Synthetic Fibers, International journal of Mechanical Engineering, vol-2, issue-2, pp-59-69, 2014
- [18] LIU Wu-fa and LI Su-yan (2012). "Analysis and Design of Steel Wire Cold Drawing-Peeling New Device" 2nd International Conference on Materials, Mechatronics

- and Automation, Lecture Notes in Information Technology, Vol.15, 84-88.
- [19] Norasethasopon, S. and Yoshida, K. (2003). "Influence of an Inclusion on Multipass Copper Shaped-Wire drawing by 2D Finite element Analysis' IJE Transactions Vol. 16, No.3, 279-292
- [20] E. KRSTI and B. LELA (2010). "Continuous Roll Casting of Aluminium Alloy- Casting Parameters Analysis" METALURGIJA 49 (2010) 115-118
- [21] Gui'e Xe, Feng Fag and Zhaoxia Li (2009). "Optimization of wire technology based on finite element modeling" Modern applied science, Vol. 3 193-198.
- [22] Jingde, Z., Hyuck-Cheol, K., Hak-Young Kim, and Sang-Min, B. (2005). "Micro-cracking of low carbon steel in hot-forming processes" Journal of Materials Processing Technology 162-163 (2005) 447-453
- [23] Changhyun, P., Seho, C., Homoon, B., Hwawon, H., Dongyeop, K. and Sangcheul, W (2008). "Development of Surface Inspection System for Wire Rod" 17th IFAC World Congress (IFAC'08) Seoul, Korea, July 6-11, 2008 6721-6722
- [24] Kesavulu, P and Ravindraredddy, G. (2014). "Analysis and optimization of wire drawing process" International Journal of Engineering and Technology, Vol 3, 635-638
- [25] D. Salcedo, C. J Luis, J. Leon, R. Luri, I. Perez (2010). "Analysis of residual stresses in wire drawing process" 14th International Research/Expert Conference, TMT 2010, 69-72.
- [26] WANG Rui-xue, Li Chun-kun and YANG jing-rui (2012). "Wire drawing Process Simulation of Polycrystalline Diamond wire drawing Die" IEEE, 212-218
- [27] Tang, K. K., Z. X. Li and J. Wang (2011). "Numerical Simulation of Damage Evolution in Multi-Pass Wire Drawing Process and its Applications" Materials and Design, 32, 3299-3311.
- [28] Sadiq Muhsin Ihmood (2011) "Calculation of Lubrication Film Thickness in Wire drawing Process" Journal of Thi-Qar University, No.1 Vol.7 41-49.
- [29] Husain Mehdi, R.S. Mishra, Mechanical properties and microstructure studies in Friction Stir Welding (FSW) joints of dissimilar alloy- A Review, Journal of Achievements in Materials and Manufacturing Engineering 77/1 (2016) 31-40.
- [30] Husain Mehdi, R.S. Mishra, Influences of Process Parameter and Microstructural Studies in Friction Stir Welding of Different Alloys: A Review, International Journal of Advanced Production and Industrial Engineering, IJAPIE-SI-MM 509 (2017) 55-62.
- [31] Radojevic, M., Radojicic, M., Nakic, M. and Babic, M. (2000). "Lubricant as parameter of processing Tribomechanical System in the Process of Wire Drawing" Tribology in industry, vol.22, No.1&2, 23-27
- [32] Kyung-hun, L. Sang-Kon, L. and Byung-Min, K. (2012). "Advance Simulation of Die wear caused by wire vibration during Wire drawing process" Science Direct, Trans, Nonferrous Met. Soc. China 22, 1723-1731
- [33] Singh, S. K., Gautham, B.P. Joshi, A. and Gudadhe, D (2007). "Development of Virtual wire drawing tool for process analysis and optimization" Wire drawing Journal, 72-78
- [34] Liu Lihua, Sun Jie, Wang Huan (2013). "Failure Analysis of Steel Wire Drawing Fracture" 13th International Conference on fracture, June 16-21 1-7.
- [35] Roger N. Wright (2011) "Wire technology: process engineering and metallurgy.
- [36] Husain Mehdi, R.S. Mishra, Mechanical and microstructure characterization of friction stir welding for dissimilar alloy- A Review, International Journal of Research in Engineering and Innovation, vol-1, issue-5, 57-67.